

Projecting a Regular Grid onto a Sphere or Ellipsoid

Rune Aasgaard

SINTEF Applied Mathematics, PO.Box 124, N-0314 Oslo, Norway,
rune.aasgaard@sintef.no

Abstract

This paper presents a new map projection intended for mapping regular Level-of-Detail structures like quad-trees, wavelets or Lindstrom/ROAM triangulations on a spherical/ellipsoidal earth. The projection maps the squares of regular structures to near-squares on the globe, even near the poles. The projection gives simple equations, visually pleasing graphic output and works well with familiar algorithms and data structures.

Keywords: global grid, cartographic projection, level-of-detail, spatial reference system

1 Introduction

In many applications, geographical data is stored as a regular quadratic grid. The data unit is a near quadratic cell. When only a limited area is handled, this grid is usually oriented to a map projection.

For global applications however, we have the problem that no projection handles the whole earth very well without having areas where the scale shows strong variation. There are discontinuities and shape or area distortions.

For a global grid of dimension COLS×ROWS a common method is to use a simple uniform scaling from the geographical coordinates, giving grid positions:

$$x = \frac{COLS}{2\pi} \lambda \quad y = \frac{ROWS-1}{\pi} (\phi + \lambda / 2) \quad (1)$$

Where the latitude domain is: $\phi \in [-\pi/2, \pi/2]$, and for the longitude: $\lambda \in [0, 2\pi>$ where λ wraps around at 2π .

This method has some advantages and several disadvantages. It is very simple, and for equatorial areas, it gives reasonable results. However, as we approach the

poles the cells on the sphere are increasingly narrower and more trapezoidal in shape.

In a Level-of-Detail (LOD) environment (for Lindstrom triangulations, terrain texture pyramids, wavelets, quad-trees etc. ...) it is often important that the aspect ratio of the cells is as close to 1 as possible. The length of the longest axis of the cell usually determines the detail level for a cell. Where the ratio between the cell dimensions is very far from 1 we would get an unnecessarily high data density in the direction where the cells are shorter.

In spite of this, the uniform scaling is frequently used in systems for global mapping. Examples are the tessellations used for GeoVRML (Reddy M, Leclerc YG, Iverson L, Bletter N (1999) or VGIS(Lindstrom P, Koller D, Ribarsky W, Hodges LF, Op den Bosch A, Faust N (1997). It is also used as the storage coordinate system of many publicly available global data sets:

- GTOPO30 (<http://edcdaac.usgs.gov/topo30/topo30.html>),
- Globe (<http://www.ngdc.noaa.gov/seg/topo/globe.shtml>).

Using a conformal map projection would correct some of this, but a conformal projection cannot map the whole earth in one projection system without having areas where the scale approaches infinity. However, continuous LOD methods allows the model to adapt to changing detail requirements over the area, and compensates for some of the large variations of scale implied with conformal projections.

Some large scale (but not global) data sets use conformal projections:

- the Smith-Sandwell bathymetric model uses the Mercator projection between 72°N and 72°S (http://topex.ucsd.edu/marine_topo/mar_topo.html), and,
- the IBCAO arctic ocean bathymetric model uses a polar stereographic projection: (<http://www.ngdc.noaa.gov/mgg/bathymetry/arctic/arctic.html>).

Other authors have gone in the opposite direction (Tobler W, Chen ZT (1986) and (Otto P (2001), defining an equal-area co-ordinate system for preserving the area of the cells instead of the shape. This approach has the advantage of having an equal data volume in each cell at the same level of detail, given a uniform complexity.

There have been other attempts to develop global grid systems based on approximating the sphere to a regular polyhedron. A prominent example is octahedral Quaternary Triangular Meshes (Dutton G (1990) and several other papers of the same author). It is based on a hierarchical decomposition of equal-sided triangles where a triangle is split into four smaller triangles for each level of detail. Other authors, for example: (Goodchild MF, Shiren Y (1992) and (Bartholdi JJ, Goldsman P (2001) have explored the QTM with emphasis on its use for spatial indexing and its geometrical properties.

The QTM gives a very homogeneous hierarchical mesh, but its triangle based split pattern makes it difficult to integrate with the commonly used square based methods. In addition, if it should be used for continuous view dependent LOD we

will need non equal-sided triangles for the connections between triangles at different levels. This breaks much of the elegance of the original model.

For global wavelets both (λ, ϕ) parameterisations (Freedman W, Windheuser U (1994) and QTM methods (Schröder P, Sweldens W (1995) have been used.

In 2000 the U.S. National Center for Geographic Information and Analysis arranged a conference on global grid structures: International Conference on Discrete Global Grids (<http://www.ncgia.ucsb.edu/globalgrids/index.html>). Several of the mentioned methods were addressed there, but there does not seem to be any general agreement on a universally "best" method.

2 Mercator's Projection

An infinitesimal change in geographic position is mapped via Mercator's projection to an infinitesimal distance on the surface of the earth ellipsoid by the following equations:

$$du = N(\phi) \cos(\phi) d\lambda, \quad dv = M(\phi) d\phi$$

Where $M(\phi)$ is the Meridial radius of curvature and $N(\phi)$ is the Normal radius of curvature:

$$N(\phi) = \frac{r_{eq}}{W(\phi)}$$

$$M(\phi) = \frac{r_{eq}(1-\varepsilon^2)}{W(\phi)^3} = N(\phi) \frac{1-\varepsilon^2}{W(\phi)^2}$$

$$W(\phi) = \sqrt{1-\varepsilon^2 \sin^2 \phi}$$

Where r_{eq} is the equatorial radius of the ellipsoid and ε is the eccentricity.

In Mercator's projection the east/west transform is defined as $x=r_{eq} \lambda$ and the north/south transform is defined so that the projection is conformal ($dx/dy=du/dv$):

$$dy = \frac{dv}{du} dx = \frac{M(\phi) d\phi}{N(\phi) \cos(\phi) d\lambda} r_{eq} d\lambda = \frac{r_{eq}(1-\varepsilon^2)}{(1-\varepsilon^2 \sin^2 \phi) \cos \phi} d\phi \quad (2)$$

In the spherical case $\varepsilon=0$ and the equation simplifies to:

$$dy = \frac{r_{eq}}{\cos \phi} d\phi \quad (3)$$

The projection transform functions are found by integrating Eqs. 2 or 3.

3 A Finite Near-Conformal Regular Grid Projection

When mapping a rectangular grid to the sphere we still want the meridians to be mapped to vertical grid lines:

$$dx=c \cdot d\lambda \quad (4)$$

In the north/south direction we want a transform that to some degree grows like the Mercator's projection, but maps to a finite range. We try a polynomial expansion of Eq. 3:

$$dy = \frac{a \cdot d\phi}{1 - (b\phi)^2} \quad (5)$$

This can be integrated to find a relation between y and ϕ :

$$y = \int_0^\phi \frac{a \cdot d\phi}{1 - (b\phi)^2} = \frac{a}{2b} \ln \left| \frac{b\phi + 1}{b\phi - 1} \right| \quad (6)$$

The parameters a and b are determined to let the projection have the properties we desire for scaling and range. From Eq. 5 we see that $dy/d\phi \rightarrow \infty$ if $b\phi \rightarrow \pm 1$. To avoid asymptotic behaviour within the ordinary range of ϕ we want $|b\phi| < 1$ for all $\phi \in [-\pi/2, \pi/2]$. Therefore $b \in \langle -2/\pi, 2/\pi \rangle$. As the equations are symmetric for positive and negative b we concentrate on $b \geq 0$.

The case $b = 0$ results in $dy = a \cdot d\phi$, and is trivial. For $b \rightarrow 2/\pi$ the scaling $dy/d\phi$ gets increasingly steeper and approaches the behaviour of the Mercator's projection. We still want a finite range for the projection, and expect a value of b that is slightly smaller than $2/\pi$.

In the following we use a domain $\phi \in [-\pi/2, \pi/2]$ and a range of $y \in [-y_{\pi/2}, y_{\pi/2}]$. We insert the values for the extremes and use a substitution for b :

$$b = \frac{2}{\pi}(1 - \delta)$$

$$y_{\pi/2} = \frac{a\pi}{4(1 - \delta)} \ln \left| \frac{2/\delta - 1}{2/\delta + 1} \right|$$

Considering the expected domain of b we would similarly expect $\delta \in \langle 0, 1 \rangle$, with the most useful value near 0. Then we can remove the absolute value symbol, and rewrite the equation as:

$$\delta = \frac{2}{1 + e^{\frac{4(1-\delta)}{a\pi} y_{\pi/2}}} \quad (7)$$

which is easily solved numerically by fixed-point iteration starting with $\delta_0 = 0$. Since the exponent over e is always positive the denominator is always greater than 2, and the restriction on δ is followed. We should note that this relation always has a solution for $\delta = 1$. Whether it also has a solution for $\delta \in \langle 0, 1 \rangle$ depends on the value of $4y_{\pi/2}/a\pi$. It is relatively easy to prove that this solution exists and is unique when:

$$y_{\pi/2} > a\pi/2 \quad (8)$$

The inverse projection is easily computed when we know that $|b\phi| < 1$:

$$\begin{aligned} e^{\frac{2b}{a}y} &= \frac{1+b\phi}{1-b\phi} \\ \phi &= \frac{e^{\frac{2b}{a}y} - 1}{e^{\frac{2b}{a}y} + 1} \left(\frac{1}{b}\right) = \frac{1}{b} \tanh\left(\frac{b}{a}y\right) \end{aligned} \quad (9)$$

3.1 Scale

The dimension of the cells are defined by du/dx and dv/dy :

$$\frac{du}{dx} = \frac{N(\phi)\cos(\phi)d\lambda}{c \cdot d\lambda} = N(\phi)\cos(\phi)/c \quad (10)$$

$$\frac{dv}{dy} = \frac{M(\phi)d\phi}{a \cdot d\phi} = \frac{M(\phi)(1-(b\phi)^2)/a}{1-(b\phi)^2} = \frac{M(\phi)}{a \cdot \cosh^2(\frac{b}{a}y)} \quad (11)$$

In the following dv/dy is called the y -scale: s_y

The aspect ratio of a cell is then:

$$\theta(\phi) = \frac{dv/dy}{du/dx} = \frac{cM(\phi)(1-(b\phi)^2)}{aN(\phi)\cos\phi} = \frac{c(1-\varepsilon^2)(1-(b\phi)^2)}{a(1-\varepsilon^2\sin^2\phi)\cos\phi}$$

The aspect ratio tells us how close the cells are to be quadratic. A value of 1 represents a quadratic cell, higher values indicate a “narrow” cell and lower values a “wide” cell. If we want the aspect ratio to be 1 at $\phi=0$ we get $a = c(1-\varepsilon^2)$.

3.2 Distance, Direction and Area

The length of an infinitesimal line element is given as:

$$\begin{aligned}
dS^2 &= du^2 + dv^2 = \left(\frac{N(\phi)\cos\phi}{c} dx \right)^2 + \left(\frac{M(\phi)(1-(b\phi)^2)}{a} dy \right)^2 \\
&= \frac{M(\phi)^2(1-(b\phi)^2)^2}{a^2} \left(\frac{dx^2}{\theta(\phi)^2} + dy^2 \right) = s_y(\phi)^2 \left(\frac{dx^2}{\theta(\phi)^2} + dy^2 \right)
\end{aligned} \tag{13}$$

The direction (azimuth, angle between the north direction and the line) of the line element:

$$\tan(Az) = \frac{du}{dv} = \frac{aN(\phi)\cos\phi}{cM(\phi)(1-(b\phi)^2)} \frac{dx}{dy} = \frac{1}{\theta(\phi)} \frac{dx}{dy} \tag{14}$$

The area of a rectangular element:

$$\begin{aligned}
dA &= du \cdot dv = \frac{N(\phi)\cos\phi \cdot M(\phi)(1-(b\phi)^2)}{c \cdot a} \cdot dx \cdot dy \\
&= \frac{M(\phi)^2(1-(b\phi)^2)^2}{a^2} \cdot \frac{dx}{\theta(\phi)} \cdot dy = s_y(\phi)^2 \cdot \frac{dx}{\theta(\phi)} \cdot dy
\end{aligned} \tag{15}$$

3.2.1 Distance Approximation

Returning to the distance calculation we introduce Eq. 14 into Eq. 13 to eliminate dx .

$$dS = s_y(\phi) \sqrt{\frac{dx^2}{\theta(\phi)^2} + dy^2} = s_y(\phi) \sqrt{\tan^2(Az) + 1} \cdot |dy| = \frac{s_y(\phi)}{|\cos(Az)|} |dy|$$

To develop a simplified equation for the length of a geodetic line we introduce some approximations that are valid for smaller distances, where some of the properties are considered constant along the line:

- Azimuth is constant along the line, and approximated as:
 $\tan(Az) = \frac{\Delta x}{\theta(\phi)\Delta y}$ then also $|\cos(Az)| = \frac{|\Delta y|}{\sqrt{\frac{\Delta x^2}{\theta(\phi)^2} + \Delta y^2}}$
- $M(\phi)$ is constant for small changes of latitude.
- $\theta(\phi)$ is nearly constant for small changes of latitude, except near the poles.

$$\begin{aligned}
S &= \int_{p_1}^{p_2} dS = \int_{y_1}^{y_2} \frac{s_y(\phi)}{|\cos Az|} |dy| = \int_{y_1}^{y_2} \frac{M(\phi)}{a|\cos Az| \cosh^2\left(\frac{b}{a}y\right)} |dy| \\
&\approx \frac{M(\phi)}{a|\cos Az|} \int_{y_1}^{y_2} \frac{|dy|}{\cosh^2\left(\frac{b}{a}y\right)} = \frac{M(\phi)}{b|\cos Az|} \left| \tanh\left(\frac{b}{a}y_2\right) - \tanh\left(\frac{b}{a}y_1\right) \right|
\end{aligned}$$

This is again expanded to the second degree in a Taylor series around $y = y_0$ (and $\phi = \phi_0$), and the approximation for $\cos(Az)$ is inserted. By selecting $y_0 = (y_1 + y_2)/2$ the second degree terms disappear and we get:

$$S = \frac{M(\phi_0)}{a \cdot \cosh\left(\frac{b}{a}y_0\right)^2} \sqrt{\frac{\Delta x^2}{\theta(\phi_0)^2} + \Delta y^2} \quad (16)$$

3.2.2 Area Approximation

The area of a grid cell is found by integrating Eq. 15 and using the same simplifications as in section 3.2.1:

$$A = \int_{x_{\min}}^{x_{\max}} \int_{y_{\min}}^{y_{\max}} \frac{M(\phi)^2}{a^2 \cosh^4\left(\frac{b}{a}y\right) \theta(\phi)} dx dy \approx \frac{M(\phi)^2 \Delta x}{a^2 \theta(\phi)} \int_{y_{\min}}^{y_{\max}} \frac{dy}{\cosh^4\left(\frac{b}{a}y\right)}$$

When using a Taylor series expansion around y_0 in the same way as above we get:

$$A = \frac{M(\phi)^2 \Delta x \cdot \Delta y}{a^2 \theta(\phi) \cosh^4\left(\frac{b}{a}y_0\right)} \quad (17)$$

4 Examples

In this section we will develop the equations further for a $2^n \times 2^m + 1$ grid. Here we get this range: $0 \leq x < 2^n$, $-2^m/2 \leq y \leq 2^m/2$. For simplicity we assume a spherical earth, the elliptical equations are developed with slightly more work from the full equations in section 3.

The east/west transform is:

$$x = \frac{2^n}{2\pi} \lambda$$

If we set the aspect ratio at equator to 1 we get $a=c=2^n/2\pi$. Given the range of y we have $y_{\pi/2}=2^m/2$.

The fix point recurrence relation is then:

$$\delta_0 = 0, \delta_{k+1} = \frac{2}{1 + e^{(1-\delta_k)2^{(m-n+2)}}}$$

and has a solution other than $\delta=1$ if (from Eq. 8):

$$1 < \frac{2y_{\pi/2}}{a\pi} = \frac{2 \cdot 2^m / 2}{\frac{2^n}{2\pi} \pi} = 2^{m-n+1} \Leftrightarrow m > n-1$$

If the grid has relative dimensions of $m = n-1$ we get $b = 0$ and a uniform scaling as in Eq. 1.

For $m > n-1$ the other equations are:

$$\begin{aligned} b &= \frac{2}{\pi}(1-\delta) \\ dy &= \frac{2^{n-1} d\phi}{\pi - (b\phi)^2} \\ y &= \frac{2^{n-3}}{1-\delta} \ln \frac{1+b\phi}{1-b\phi} \\ \phi &= \frac{1}{b} \cdot \tanh\left(\frac{1-\delta}{2^{n-2}} y\right) \\ \theta(\phi) &= \frac{1-(b\phi)^2}{\cos \phi} \end{aligned}$$

4.1. Aspect ratio

As the aspect ratio $\theta(\phi)$ is important for the shape of the grid cells it is studied in more depth. For the limit case $m=n+\infty$, $b = 2/\pi$ the aspect ratio is:

$$\theta_{m=n+\infty}(\phi) = \frac{1 - \left(\frac{2}{\pi} \phi\right)^2}{\cos \phi}$$

This can be considered the "best" aspect ratio that can be obtained by this method. It has its maximum at $\theta(\pi/2) = 4/\pi$. Naturally, for a conformal projection the aspect ratio would be constant 1 for the whole domain.

Some computations of aspect ratios are summarised in Fig. 1. Except for the limit case the aspect ratio rises to infinity at the poles. The size of the grid cells (the projection scale) would also change dramatically from cell to cell as we

approach the pole. As expected, the projection is not well suited if the area of interest is very close to the poles.

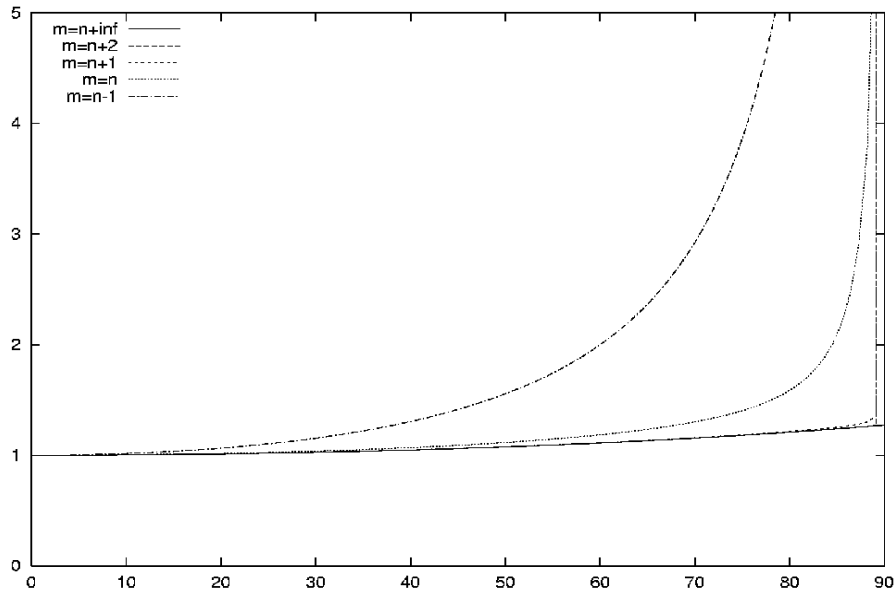


Fig. 1. Aspect ratios for different values of $m=n+x$

However, for $m = n+1$ the aspect ratio is reasonable even a few ten kilometers from the pole and for $m = n+2$ it is still less than 1.5 at around 100m from the pole.

For many applications an aspect ratio of around 2 at 85° is acceptable, at least much better than an aspect ratio of 2 at 60° as the uniform scaling would give. At the same time the quadratic coordinate range we get when $m=n$ may have advantages by using the coordinate values most efficiently.

The improvement given by going from $m=n+1$ to $m=n+2$ may not be worth the extra narrowing of the x coordinate range. Instead it may have some advantages to change the scaling (parameter a) so that the aspect ratio at the equator is slightly less than 1, to distribute the error more evenly.

4.2 Approximation Errors

When using the approximated equations for distance or grid cell area we would like to know their area of acceptable accuracy. This is not necessarily easily computed, as it may be difficult to estimate the impact of the simplifications in the development of the approximated equations.

The errors are found by comparing distances computed with the approximated equations and "exact" geodetic line methods. A series of computations is

performed with successively larger distances until the error reaches a given threshold. Fig. 2. shows the maximum distance in kilometers before the error threshold is reached, at different latitudes.

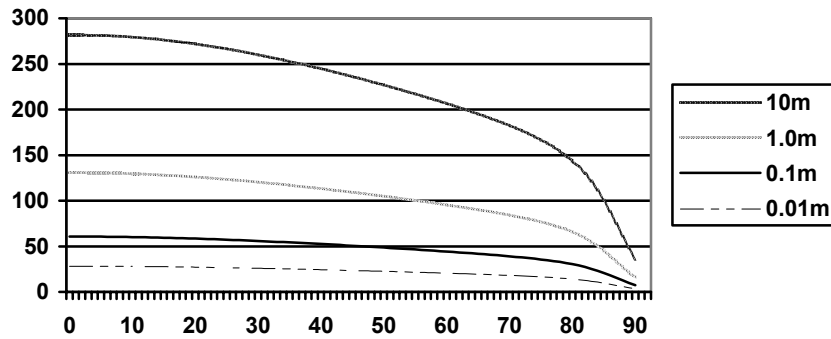


Fig. 2. Approximation error thresholds in distance computation, $m = n$ grid

As expected, the maximum distance for a given error tolerance is reduced with increasing latitude. In this case, the distances are computed for a line with azimuth 135° , for longer distances, the error is direction dependent, and using another direction would give slightly different results. Similar tables can also be computed for the area approximation, comparing the results with data from the Lamberts equal-area projection.

5 Conclusion

For data visualisation purposes, the global regular grid projection is capable of mapping a regular grid to the globe with acceptable distortions. It has two singularities - at the poles - and most of the projection distortions are concentrated there. As the scale increases towards the poles a grid cell covers successively smaller area. This implies an increasing resolution towards the poles. For most purposes, however, the interesting data is located in the lower latitudes, and the projection should preferably be combined with a LOD structure for balancing the scale with the need for resolution.

The projection is relatively simple to integrate with many well-known methods and data structures. More complex methods may give better results, but are usually considered too difficult for practical use. Most projects therefore fall back to using a uniform scaling to latitude/longitude. For them, this method could be a good alternative.

For limited regions, various geometrical properties like distance and area can be computed directly from projected grid coordinates. The approximation error

thresholds are not easily found, and a table area size, where the error is within acceptable limits, should be computed before the approximation functions are used.

The projection is used in a "virtual globe" project on the Internet where a Lindstrom/ROAM-like regular triangulation is mapped to the earth, described in (Aasgaard R, Sevaldrud T (2001). The methods are demonstrated on <http://globe.sintef.no>.

As an example two regular partition triangulations are shown in Fig. 3.

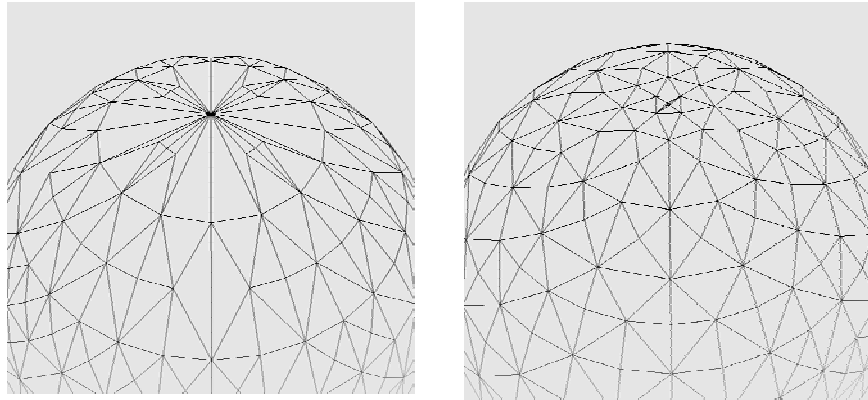


Fig. 3. Uniform scaling (left) vs. $m=n+1$ projection (right).

Acknowledgements

The Research Council of Norway through the DynaMap project and the European Union through the TellMaris project have supported this work.

References

- Aasgaard R, Sevaldrud T (2001) Distributed handling of level of detail surfaces with binary triangle trees. Proceedings of ScanGIS'2001
- Bartholdi JJ, Goldsman P (2001) Continuous indexing of hierarchical subdivisions of the globe. *International Journal of Geographical Information Science* 15(6): 489-522
- Bugajevsky LM, Snyder JP (1995) *Map Projections, A Reference Manual*. Taylor & Francis
- Dutton G (1990) Locational properties of quaternary triangular meshes. *Proc. Spatial Data Handling Symp.* 4. July, 1990, Dept. of Geography, U. of Zurich, pp 901-910
- Freedon W, Windheuser U (1994) *Spherical Wavelet Transform and its Discretization*. Tech. Rep. 125, Universität Kaiserslautern, Fachbereich Mathematik
- Goodchild MF, Shiren Y (1992) A hierarchical spatial data structure for global geographic information systems. *Computer Vision, Graphics and Image Processing* 54(1): 31-44

- Lindstrom P, Koller D, Ribarsky W, Hodges LF, Op den Bosch A, Faust N (1997) An Integrated Global GIS and Visual Simulation System. Technical report GIT-GVU-97-07, March 1997
- Ottoson P (2001) Retrieval of geographic data using elliptical quadtrees. Proceedings of ScanGIS'2000
- Reddy M, Leclerc YG, Iverson L, Bletter N (1999) TerraVision II: Visualizing Massive Terrain Databases in VRML. IEEE Computer Graphics and Applications (Special Issue on VRML) 19(2): 30-38
- Schröder P, Sweldens W (1995) Spherical wavelets: Efficiently representing functions on the sphere. University of South Carolina Department of Mathematics: Columbia, S.C. Industrial Mathematics Initiative 1995:01
- Tobler W, Chen ZT (1986) A quadtree for global information storage. Geographical Analysis 18(4): 360-371